Mantle wedge dynamics vs crustal seismicity in the Apennines (Italy)

Guido Ventura[1], Francesca R. Cinti[1], Francesca Di Luccio[1], N. Alessandro Pino[2]

[1]Istituto Nazionale di Geofisica e Vulcanologia, Department of Seismology and Tectonophysics, Rome, Italy

[2]Istituto Nazionale di Geofisica e Vulcanologia, Osservatorio Vesuviano, Naples, Italy

Abstract In the Apennines subduction (Italy), earthquakes mainly occur within overriding plate, along the chain axis. The events concentrate in the upper 15 km of the crust above the mantle wedge and focal solutions indicate normal faulting. In the foreland, the seismogenic volume affects the upper 35 km of the crust. Focal solutions indicate prevailing reverse faulting in the northern foreland and strike-slip faulting in the southern one. The deepening of the seismogenic volume from the chain axis to the foreland follows the deepening of the Moho and isotherms. The seismicity above the mantle wedge is associated with uplift of the chain axial zone, volcanism, high CO_2 flux, and extension. The upward pushing of the asthenospheric mantle and the mantle-derived, CO_2-rich fluids trapped within the crust below the chain axis causes this seismicity. All these features indicate that the axial zone of Apennines is affected by early rifting processes. In northern Italy, the widespread and deeper seismicity in the foreland reflects active accretion processes. In the southern foreland, the observed dextral strike-slip faulting and the lack of reverse focal solutions suggest that accretion processes are not active at present. In our interpretation of the Apennines subduction, the shallower seismicity of the overriding plate is due to the dynamics (uprising and eastward migration) of the asthenospheric wedge.

Keywords: Apennines, crustal seismicity, rifting, subduction, fluids, geodynamics

Index terms: 8120 Dynamics of lithosphere and mantle: general; 7230 Seismicity and tectonics; 8045 Role of fluids; 7240 Subduction zone; 8109 Continental tectonics: extensional.

1. Introduction

The seismicity of the Apennines subduction (Italy) concentrates in the overriding plate at shallow (<40 km) depth. Fewer and deeper earthquakes reach 90 km depth and locate below the northern sector of the Apennines chain (Fig. 1). These features are unusual in subduction settings, where the earthquakes prevalently occur in the downgoing plate or, as in Japan, in both the downgoing and overriding plates [*Stern*, 2002].

The geodynamic significance of the crustal seismicity in the Apennines subduction is still poorly known. Most studies focus on relatively small areas to infer the local (~10^2-10^4 km^2 scale) seismotectonic setting [e.g., *Chiaraluce et al.*, 2004; *Eva et al.,* 2005], while larger scale studies [*Chiarabba et al.,* 2005] analyze the whole seismicity of Italy and do not detail the shallow earthquakes of the Apennines. Some authors [*Ghisetti and Vezzani*, 2002; *Chiodini et al.*, 2004] discuss the role of the CO_2 degassing in triggering the seismicity of the Apennines. In these studies, however, the relationship among CO_2 degassing, volcanism, and the geodynamic evolution of the Apennines and surrounding regions is not analyzed.

Here we study the spatial distribution and focal solutions of the crustal earthquakes that occurred in the Apennines and surrounding regions in the 1981-2002 period. We merge these data with tomographic images, CO_2 measurements, depth of the Moho, stress and GPS measurements, and geochemical features of the Quaternary volcanism. The processes responsible for the Apennines seismicity are investigated and a geodynamic model of the Apennines subduction is proposed.

2. Geodynamic setting

The Neogene Apennines fold-and-thrust belt represents the accretionary wedge of a subduction zone that includes the Tyrrhenian back-arc and the Adriatic-Apulian foreland and foredeep (Fig. 1A, B). From Tortonian times, the thrust front migrates northeastward due to the rollback of a west dipping slab and the back-arc opened to the west [*Malinverno and Ryan,* 1986]. The Apennines belt consists of two main segments: the arc-shaped Northern Apennines, and the NW-SE striking Southern Apennines (Fig. 1A). This different configuration reflects the larger hinge rollback rate of the northern, 70 km thick Adriatic lithosphere with respect to the southern, 110 km thick, Apulian lithosphere [*Doglioni et al., 1994*]. The Late Pliocene-Pleistocene geodynamics of the inner and axial sectors of the Apennines is characterized by a NE-SW striking extension associated with uplift [values up to 2.5-3.0 mm/yr; *D'Anastasio et al.,* 2006], volcanism, high CO_2 and heat flux [*Montone et al.,* 2004; *Bartolini et al.,* 2003; *Chiodini et al.,* 2004]. This extension is responsible for the NW-SE striking normal faults that affect the axial zone of the Apennines and bound the main intermountain basins. Compression is confined in the foreland. The Adriatic foreland is subsiding from Pleistocene times whereas the Apulian foreland is uplifting (Fig. 2) [*Doglioni et al.,* 1994].

The crustal thickness increases from 15 to 25 km moving from the Tyrrhenian Sea to the chain axis, and reaches 30-35 km in the foreland (Fig. 2). A local thickening (up to 45-50 km) of the Adriatic Moho beneath the Northern Apennines was found by *Mele and Sandvol* [2003] along a transect located between the profile B-B' and C-C' of Fig. 2. Beneath the Apennines axis, gravity and seismic data identify a doubling of the Moho (Figs. 4 and 5) [*Locardi and Nicholich,* 1988; *Finetti et al.,* 2001; *Tiberti et al.,* 2005]. According to shear wave attenuation studies [*Mele et al.,* 1997], surface wave tomography [*Panza et al.,* 2003], and gravity data [*Tiberti et al.,* 2005], this doubling of Moho is interpreted as a 'soft' asthenospheric wedge intruding between the downgoing Adriatic plate and the overriding plate. CO_2 flux data [*Chiodini et al.,* 2004] indicate that the inner and axial sectors of the Apennines are affected by a diffuse degassing (areas with CO_2 flux> 0.5 $td^{-1}km^{-2}$in Fig. 2) whose spatial distribution well exceeds that of the volcanic areas. The origin of CO_2 is, according also to $^3He/^4He$ values [*R*/*Ra* up to 4.48; *Minissale,* 2004], from a prevailing deep mantle source with minor contributions of crustal and organic components. Plio-Quaternary volcanism characterizes the inner sectors of Apennines (volcanoes of Tuscany, Latium and Campania in Fig. 2) as well as some axial sectors of the chain (volcanoes of Umbria and Vulture). These volcanoes are located where the crustal thickness is less than 30 km and their products belong to the K-alkaline, calcalkaline and shoshonitic associations [*Peccerillo*, 2005 and reference therein].

Tomographic images of the Apennines-Tyrrhenian Sea region [*Piromallo and Morelli*, 2003] show a subvertical, W-dipping slab beneath the chain (Fig. 1B). However, these images do not resolve the issue of the occurrence or not of a slab detachment [see *Carminati et al.,* 2002 for a discussion]. Based on petrologic data, *Lavecchia et al.* [2003] and *De Astis et al.* [2006], suggest that the subduction is ceased and the slab is detached. On the contrary, *Doglioni et al.* [1999] and *Carminati et al.* [2002] propose that the rollback is still active. Following this interpretation, the lack of deep seismicity below the Apennines is due to ductile deformation of the quartz-feldspar rich subducting continental lithosphere coupled to low subduction rates and to a ‘hot’ asthenospheric mantle wedge.

The deep (up to 500 km) seismicity of the Southern Tyrrhenian Sea-Calabrian Arc region (Fig. 1A), and the calcalkaline character of the volcanism, is due to the active rollback of a NW-dipping slab.

3. Crustal seismicity

We analyze the spatial distribution and rupture processes of the crustal (depth <40 km) events occurred in the period 1981-2002 and selected according to the hypocentral and horizontal errors (<4 km) and the root mean square residuals (<0.8 s) [*Castello et al.,* 2005; *Chiarabba et al.*, 2005]. Focal mechanisms are from Regional Centroid Moment Tensor (RCMT) catalog (http://mednet.rm.ingv.it/rcmt/rcmt.htm) for events with $M_l \geq 4.5$. For earthquakes with $3.5 \leq M_l < 4.5$, moment tensor solutions are automatically computed inverting the full high-quality broadband waveforms recorded at the Mediterranean Seismic Network operated by The Istituto Nazionale di Geofisica e Vulcanologia (Rome, Italy). Details about the technique and the automatic moment tensor solutions can be found in *Di Luccio et al.* [2005a] and at http://mednet.rm.ingv.it/events/Welcome.html.

Earthquakes concentrate along the Apennines axial zone, where they define a 50 to 80 km wide seismic belt (Fig. 2). Scarce seismicity characterizes the inner sector of the chain and the few events are in geothermal/volcanic areas. To the east of the chain, the seismicity is widespread, except for some locations, where E-W to ENE-WSW oriented, 20 to 50 km wide bands extend from the chain axis to the foreland (profiles A-A' to E-E' in Figs. 2, 4 and 5).

As a common feature, all the sections in Figs. 4 and 5 clearly define a gradual eastward deepening of the seismicity. The profile A-A' crosses the northwestern tip of the Northern Apennines (Fig. 2 and Fig. 4). The available focal solutions show thrusts and strike-slip ruptures between 25 and 35 km of depth in the foreland.

The profile B-B' crosses the central part of the Northern Apennines (Fig. 2). Sparse shallow (depth <15-20 km) seismicity characterizes the western half of the section (Fig. 4). In the eastern half, two major seismic zones occur at different depths. The shallower one extends from 75 to 105 km along the profile and locates on the chain axis to a depth of 15 km, above the mantle wedge. At the eastern tip of the mantle wedge, the deeper cluster between 105 and 125 km along the profile, occurs in the foreland and extends in depth from 20 to 30-35 km. The focal solutions indicate shortening in the Adriatic foreland between 10 and 30 km depth. In the inner sectors of the Apennines, microearthquake focal mechanisms [*Eva et al.,* 2005] show thrust solutions below 10 km depth, but indicate normal motion along NW-SE faults within the uppermost 10 km.

The profile C-C' locates at the southern end of the Northern Apennines (Fig. 4). Areas with gaps and dense seismicity characterize this profile. The major cluster, between 80 and 100 km along the profile, occurs at a depth shallower than 15 km and is located where the CO_2 flux abruptly decreases, above the Moho doubling zone. This cluster includes a sequence that occurred in 1997 (M_l^{max}= 5.8) and was driven by a coseismic fluid pressure pulse of a deep source of a trapped high-pressure CO_2 reservoir [*Miller et al.,* 2004]. The rupture mechanisms of these earthquakes are prevalently normal (Fig. 4); the only available focal solution in the foreland indicates reverse faulting.

The profile D-D' is at the boundary between the Northern and Southern Apennines (Fig. 2). The westernmost cluster is at depth <15 km and locates where the CO_2 flux vanishes, above the Moho doubling zone (Fig. 5). Other clusters at depth <15 km occur at 60-70 km, 90-100 km and 110 km along the section. Events deeper than 15 km concentrate at 100 km eastward along the profile. From west to east, the focal solutions indicate normal faulting at 10-15 km of depth beneath the Southern Apennines, and strike-slip/reverse faulting at 15-30 km of depth in the foreland. The deeper earthquakes showing right-lateral mechanisms are referred to a sequence (M_l^{max}= 5.4) that occurred in 2002 at the outer margin of the belt [*Di Luccio et al.,* 2005a]. The beach-balls in the Apulian foreland indicate NW-SE compression. Following *Milano et al.* [2005], this compression is responsible for right-lateral strike-slip deformation along E-W faults.

In the section E-E' (Fig. 2 and Fig. 5) two main clusters occur. The westernmost one is confined in the upper 18 km, in the area where the CO_2 flux suddenly decreases, whereas the other one reaches a depth of about 30 km. Normal faulting characterizes the earthquakes within the chain, including the 1980 mainshock ($M_l = 6.5$), which was the more energetic earthquake occurred in the Apennines in the last century. A transition from normal to prevailing dextral strike-slip regime occurs between 40 and 50 km of the profile, above the Moho doubling zone. The strike-slip mechanisms are relative to the 1990-1991 sequences [$M_l^{max} = 5.2$; *Di Luccio et al.*, 2005b].

Different types and directions of the stress field characterize the Apennines chain and the external margin of the belt and foreland. Stress data indicate active extension orthogonal to the chain axis in the Northern and Southern Apennines (see black arrows in Fig. 3). This is responsible for the normal faults along the chain axis. In the outer margin of the northern belt and in the Adriatic foreland, the stress regime becomes compressive and the maximum compression axis is perpendicular to the arc curvature, where the major thrusts are mapped. The geodetic shear strain [*Hunstad et al.*, 2003] reported in Fig. 3 is consistent with the above described stress distribution along the chain axis and in the foreland. In the southern sector of the chain, a remarkable change from extension to transcurrent regime occurs at the thrust front and in the Apulian foreland, mainly along E-W dextral strike-slip faults. The focal mechanisms in the southern profiles (D-D' and E-E' in Fig. 5) demonstrate this transition from west to east occurring around 15-20 km depth. In the outer margin of the chain, the axis of maximum compression varies from NE-SW in the north to NW-SE in the south (Fig. 3).

4. Discussion

The spatial distribution of the Apennines earthquakes indicates that the crustal seismicity concentrates in the chain axis (Fig. 1). In the foreland, seismicity occurs in relatively restricted areas. The distribution of hypocenters (Figs.1, 2, 4 and 5) shows an absolute maximum at 5-7 km depth and a second-order maximum at 20-25 km. The first one links to the earthquakes occurring along the chain axis, within the overriding Tyrrhenian plate, whereas the second one relates to the events in the foreland, within the downgoing Adriatic-Apulian plate. As a result, the hypocenters deepen from the chain axis to the foreland. The 500°C isotherm, which roughly marks the brittle-ductile transition within the crust [*Ranalli and Murphy,* 1987], displays a similar behaviour (cross-sections B-B' and EE' in Figs. 4 and 5). This observation suggests that the different thickness of the seismogenic volume in the chain and in the foreland is due to differences between the thermal layering of the crust beneath the Apennines (Moho depth ~25 km; heat flow =60-140 mWm^{-2}), and beneath the Adriatic foreland (Moho depth ~35 km; heat flow <60 mWm^{-2}) [*Zito,* 2005].

The shallower (depth <15 km) events in the Apennines axial zone concentrate where the CO_2 flux decreases (Figs. 2, 4 and 5), i.e., where the mantle wedge intrudes between the Adriatic and the Tyrrhenian plates. For these earthquakes, the available focal mechanisms indicate normal faulting (Fig. 3). As suggested by *Ghisetti and Vezzani* [2002] for the Northern Apennines, the CO_2 released from the mantle wedge uprises along low permeability, presently inactive Pliocene thrusts. Overpressure within these traps may favour earthquakes and normal faulting [*Chiodini et al.*, 2004; *Miller et al.,* 2004].

In the Apennines, the coexistence of (a) seismicity and normal faulting concentrated along the chain axis, (b) uplift, (c) volcanism, and (d) diffuse CO_2 degassing, call for an active, early rifting process. We propose that this rifting process of the Apennines axial zone is due to the uprising of the mantle wedge, which is the main source of the CO_2-rich fluids. In this frame, we believe that the shallower seismicity of the chain reflects the response of the continental crust to the dynamics of the underlying asthenospheric mantle. According to this interpretation, the geochemical features of the Plio-Quaternary volcanism of the inner sectors and axial zone of the Apennines (Vulture and volcanoes of Latium, Tuscany, Umbria, and Campania in Fig. 2) indicate a mixing between a radiogenic ($^{87}Sr/^{86}Sr$~0.717) enriched mantle (EM) source and a less radiogenic ($^{87}Sr/^{86}Sr$~0.703), high U/Pb, HIMU source [*Peccerillo and Lustrino,* 2005]. The EM source is interpreted as a mantle source modified by the addition of subducted crustal material, whereas the HIMU source reflects homogeneous asthenospheric melts. Therefore, we suggest that the composition of the mantle wedge beneath the chain results from the mixing of melts modified by subduction processes and newly added asthenospheric melts. The volcanic and CO_2 diffuse degassing zone of the Apennines is located above the mantle wedge, in the sector of the subduction where the maximum compressive stress is vertical (see Figs. 3, 4 and 5). To the east of the degassing zone, volcanoes are absent and the CO_2 flux decreases abruptly (Fig. 2). Here, the maximum compressive stress is horizontal (Figs. 3, 4 and 5). This structural configuration well agrees with that resulting from numerical models of volcanic fronts in subduction zones [*Furukawa,* 1993]. According to these models, we propose that the occurrence of (a) a vertical maximum compressive stress in the mantle wedge and (b) a large deviatoric stress in the axial zone of the Apennines allows the growth of vertical cracks along which the magma may uprise to the surface. In the Adriatic and Apulian foredeep/foreland region, the maximum compressive stress becomes horizontal, and the uprising of magma and CO_2-rich fluids is not allowed.

The uprising of the asthenospheric wedge and the compositional features of the mantle beneath the Apennines are consistent with models of slab rollback [*Doglioni,* 1991; *Gvirtzman and Nur,* 1999], which show a suction of asthenospheric material within the wedge. Accordingly, the eastward and upward pushing of the asthenosphere is responsible for the uplift and crustal thinning of the Apennines, as suggested by *Doglioni et al.* [1999], and, along with the CO_2 flux, for the crustal seismicity and extension along the chain axis (Figs. 2, 4 and 5). In this picture, we suggest that the deeper (up to 35 km) compressive earthquakes occurring at the eastern tip of the mantle wedge may reflect the local shortening of the crust in the Adriatic foredeep (e.g., section B-B' in Fig. 4). Away from the mantle wedge, the 10 to 35 km deep thrust-type earthquakes in the subsiding Adriatic foreland reflect active accretion processes. The thickness of the seismogenic volume in the Adriatic foreland is consistent with results from rheological models [*Carminati et al.,* 2002], which estimate a thickness of the brittle layer in the downgoing plate at ~ 35-40 km.

To the south, in the uplifting Apulian foreland, focal solutions (Fig. 3 and 5) and information from local studies [*Di Luccio et al.,* 2005a,b; *Milano et al.,* 2005] indicate prevailing dextral movements along E-W shears in response to a NW-SE compression. According to *Chilovi et al.* [2000], these shears represent inherited Mesozoic structures reactivated as dextral faults from Pleistocene times. The inferred direction of compression, which is parallel to the thrust front of the Southern Apennines, and the lack of reverse focal mechanisms along the chain axis allow us to conclude that the northeastward migration of the Southern Apennines thrust front is, at the present, locked. In this picture, the kinematics of the E-W shears in the Apulian foreland, where the thrust fronts of the Southern and Northern Apennines converge (Fig. 1), is due to the active northeastward propagation of the Northern Apennines front, whereas the Southern Apennines front is inactive. We propose that accretionary processes in the Southern Apennines are virtually ceased. In addition, the geochemical features (HIMU-like source) of the Vulture volcano (Figs. 2 and 5), which is located at the boundary between the Southern Apennines external front and the foredeep, indicate a mantle inflow from the Adriatic plate [*De Astis et al.,* 2006]. This feature, along with the lack of intermediate/deep earthquakes and the occurrence of a slow velocity zone between 100 and 200 km of depth below the Southern Apennines [*Piromallo and Morelli*, 2003 and references therein] suggests the presence of a ‘window’ in the Adriatic plate from which melts may uprise and differentiate within the overriding plate.

5. Conclusions

We conclude that the shallow seismicity of the Tyrrhenian-Apennines-Adriatic subduction zone is related to the dynamics of the underlying mantle wedge. At the eastern tip of the wedge, the upward and eastward migration of asthenospheric melts and CO_2-rich fluids triggers the seismicity beneath the chain axis and in the adjacent foreland. These features indicate that the Apennines chain axis is affected by active rifting processes. The uprising of asthenospheric melts, responsible for the volcanism of the chain, occurs along cracks created by a vertical maximum compressive stress in the axial zone of the Apennines. The lack of active volcanism in the Adriatic-Apulian foreland is due to a horizontal maximum compressive stress that prevents the raising of fluids within the crust. The accretion of the chain and the northeastward migration of the Apennines thrust front occur only in the northern sector, whereas these processes are inactive in the southern sector. Finally, a slab window is suggested in the Southern Apennines subduction zone.

Acknowledgements We thank C. Piromallo for the review of an early version of the manuscript, for clarifications about the mechanisms of subduction, and for the tomography section reported in Fig. 1B. We also thank G. Chiodini, G. De Astis and A. Peccerillo for the numerous discussions on the relationships between degassing processes and volcanism of Italy. Comments and suggestions by P. Lundgren, an anonymous reviewer, P. van Keken and the anonymous associated Editor helped to improve the manuscript.

References

Bartolini, C., N. D'Agostino, and F. Dramis (2003), Topography, exhumation, and drainage network evolution of the Apennines, *Episodes, 26*, 212-216.

Carminati, E., F. Giardina, and C. Doglioni (2002), Rheological control of subcrustal seismicity in the Apennines subduction (Italy), *Geoph. Res. Lett.,* doi,10.1029/2001GL014084.

Castello, B., G. Selvaggi, C. Chiarabba, and A. Amato (2005), CSI Catalogo della sismicità italiana 1981-2002, Version 1.0. *INGV-CNT, Roma*, http,//www.ingit/CSI/

Chiarabba, C., L. Jovane, and R. Di Stefano (2005), A new view of Italian seismicity using 20 years of instrumental recordings, *Tectonophysics, 395*, 251-268.

Chiaraluce, L., A. Amato, M. Cocco, C. Chiarabba, G. Selvaggi, M. Di Bona, D. Piccinini, A. Deschamps, L. Margheriti, F. Courboulex, and M. Ripepe (2004), Complex Normal Faulting in the Apennines Thrust-and-Fold Belt, The 1997 Seismic sequence in Central Italy, *Bull. . Seism. Soc. Am., 1/94*, 99-116.

Chilovi, C., J.A. De Feyter, and A. Pompucci (2000), Wrench zone reactivation in the Adriatic Block, the example of the Mattinata Fault System (SE Italy), *Boll. Soc. Geol. It., 119*, 3-8.

Chiodini, G., C. Cardellini, A. Amato, E. Boschi, S. Caliro, F. Frondini, and G. Ventura (2004), Carbon dioxide Earth degassing and seismogenesis in central and southern Italy, *Geoph. Res. Lett.*, doi,10.1029/2004GL019480.

D'Anastasio, E., P.M. De Martini, G. Selvaggi D. Pantosti, A. Marchioni, R. Maseroli (2006), Short-term vertical velocity field in the Apennines (Italy) revealed by geodetic levelling data, *Tectonophysics, 418*, 219–234.

De Astis, G., D. Kempton, A. Peccerillo, and T. Wu (2006), Trace element and isotopic variations from Mt. Vulture to Campanian volcanoes, constraints for slab detachment and mantle inflow beneath southern Italy, *Contr. Mineral. Petrol.,* doi,10.1007/s00410-006-0062-y

Della Vedova, B., S. Bellani, G. Pellis, and D. Squarci (2001), Deep temperatures and surface heat flow distribution, in G.B. Vai and Martini editors, "*The Apennines, Anatomy of an orogen*". Kluwer Academic Publishers.

Di Luccio, F., E. Fukuyama, and N.A. Pino (2005a), The 2002 Molise earthquake sequence, what can we learn about the tectonics of Southern Italy?, *Tectonophysics, 405*, 141–154.

Di Luccio, F., A. Piscini, N.A. Pino, and G. Ventura (2005b), Reactivation of deep faults beneath Southern Apennines, evidence from the 1990–1991 Potenza seismic sequences, *Terra Nova,* doi, 10.1111/j.1365-3121.2005.00653.x

Doglioni, C. (1991), A proposal for the kinematic modelling of W-dipping subductions; possible applications to the Tyrrhenian-Apennines system, *Terra Nova, 3,* 423-434.

Doglioni, C., F. Mongelli, and M. Pieri (1994), The Puglia uplift (SE-Italy), an anomaly in the foreland of the Apenninic subduction due to buckling of a thick continental lithosphere, *Tectonics, 13,* 1309-1321.

Doglioni, C., P. Harabaglia, G. Martinelli, F. Mongelli, and G. Zito (1996), A geodynamic model of the southern Apennines, *Terra Nova, 8,* 540-547.

Doglioni, C., E. Gueguen, P. Harabaglia, and F. Mongelli (1999), On the origin of W-directed subduction zones and applications to the western Mediterranean, *Geol. Soc. Am., Spec. Pap., 156*, 541-561.

Eva, E., G. Ferretti, and S. Solarino (2005), Superposition of different stress orientations in the western sector of the northern Apennines (Italy), *J. Seism., 9(4),* 413-425.

Finetti, I.R., M. Boccaletti, M. Bonini, A. Del Ben, R. Geletti, M. Pipan, and F. Sani (2001), Crustal section based on CROP seismic data across the North Tyrrhenian-Northern Apennines-Adriatic Sea, *Tectonophysics, 343*, 135–163.

Furukawa, Y. (1993), Magmatic processes under arcs and formation of the volcanic front, *J. Geophys. Res., B98,* 8309-8319.

Ghisetti, F., and L. Vezzani (2002), Normal faulting, transcrustal permeability and seismogenesis in the Apennines (Italy), *Tectonophysics, 348,* 155-168.

Gvirtzman, Z., and A. Nur (1999), Plate detachment, asthenosphere upwelling, and topography across subduction zones, *Geology, 27*, 563-566

Hunstad, I., G. Selvaggi, N. D'Agostino, P. England, P. Clarke, and M. Pierozzi (2003), Geodetic strain in peninsular Italy between 1875 and 2001, *Geophys. Res. Lett.*, *30*(4), 1181, doi:10.1029/2002GL016447.

Lavecchia, G., P. Boncio, and N. Creati (2003), A lithospheric-scale seismogenic thrust in central Italy*, J. Geodynam., 36*, 79–94.

Locardi, E., and R. Nicolich (1988), Geodinamica del Tirreno e dell'Appennino centromeridionale, la nuova carta della Moho, *Mem. Soc. Geol. It., 41* 121-140.

Malinverno, A., and B.F. Ryan (1986), Extension in the Tyrrhenian Sea and shortening in the Apennines as result of arc migration driven by sinking of the lithosphere, *Tectonics, 5,* 227-245.

Mele, G., A. Rovelli, D. Seber, and M. Baranzagi (1997), Shear wave attenuation in the lithosphere beneath Italy and surrounding regions, Tectonic implications, *J. Geophys. Res., 102(B6)*, 11863-11875.

Mele, G., and E. Sandvol (2003), Deep crustal roots beneath the northern Apennines inferred from teleseismic receiver functions, *Earth Planet. Sci. Lett., 211,* 69-78.

Merlini, S., and G. Cippitelli (2001), Structural styles inferred by seismic profiles, in G.B. Vai and Martini editors, "*The Apennines, Anatomy of an orogen*". Kluwer Academic Publishers 441-454.

Milano, G., R. Giovambattista, and G. Ventura (2005), Seismic constraints on the present-day kinematics of the Gargano foreland, Italy, at the transition zone between the Southern and Northern Apennine belts, *Geoph. Res. Lett.*, doi, 10.1029/2005GL024604

Miller, S.A., C. Collettini, L. Chiaraluce, M. Cocco, M. Barchi, and B.J. Kaus (2004), Aftershocks driven by a high-pressure CO_2 source at depth, *Nature, 427*, 724-727.

Minissale, A. (2004), Origin, transport and discharge of CO_2 in central Italy, *Earth Sci. Rev., 66*, 89-141.

Montone, P., M.T. Mariucci, S. Pondrelli, and A. Amato (2004), An improved stress map for Italy and surrounding regions (Central Mediterranean), *J. Geophys. Res.*, doi,10.1029/2003JB002703.

Panza, G., A. Pontevivo, G. Chimera, R. Raykova, and A. Aoudia (2003), The lithosphere/asthenosphere, Italy and surroundings, *Episodes, 26,* 169-174.

Peccerillo, A. (2005), *Plio-Quaternary volcanism in Italy, petrology, geochemistry, geodynamics*. Heidelberg-Springer Verlag, 365 p

Peccerillo A., and M. Lustrino (2005), Compositional variations of Plio-Quaternary magmatism in the circum-Tyrrhenian area, Deep- vs. shallow-mantle processes, *Geol. Soc. Am., Spec. Pap.,* 388, 421-434.

Piromallo, C., and A. Morelli (2003), P wave tomography of the mantle under the Alpine-Mediterranean area, *J. Geophys. Res.*, doi,10.1029/2002JB001757.

Ranalli, G., and D.C. Murphy (1987), Rheological stratification of the lithosphere, *Tectonophysics, 132,* 281-295.

Stern, R.J. (2002), Subduction zones, *Review in Geophysics*, doi 10.1029/2001RG000108.

Tiberti, M.M., L. Orlando, D. Di Bucci, M. Bernabini, and M. Parotto (2005), Regional gravity anomaly map and crustal model of the Central-Southern Apennines (Italy), *J. Geodyn., 40,* 73-91.

Zito, G. (2005), Heat flow anomaly and lithospheric thinning of the Tuscan extensional backarc basin (Italy), *J. Geodyn., 40,* 1-22.

Figure captions

Figure 1. (A) Schematic geodynamic picture of Italy and epicentral distribution of events occurred between 1981 and 2002 [data from *Castello et al.,* 2005]. (B) Tomographic section (A-A' in Fig. 1A) across the Northern Apennines [*Piromallo and Morelli,* 2003] and seismicity according to Fig. 1A. Number of events vs. distance and depth is shown (grey areas).

Figure 2. Structural map and M_l>2.0 crustal (depth < 40 km) seismicity of the study area [data from *Castello et al.,* 2005]. Dots are scaled proportionally to the magnitude. The location of the A-A' to E-E' cross sections (dashed lines) of Figs. 4 and 5 is reported. Moho isobaths are from *Locardi and Nicolich* [1988]. CO_2 flux is from *Chiodini et al.* [2004].

Figure 3. Structural map and focal mechanisms from Quick Regional Centroid Moment Tensor catalogue (http://mednet.rm.ingv.it/rcmt/rcmt.htm) and Automatic Moment Tensor solutions (http://mednet.rm.ingv.it/events/Welcome.html). Stress regime is from *Montone et al.* [2004]. The eastern boundary of the mantle wedge is from *Panza et al.* [2003]. Geodetic strain is from GPS measurements [*Hunstad et al.*, 2003].

Figure 4. Depth distribution of the seismicity of Fig. 1 on the cross-sections A-A' to C-C' shown in Fig. 2. The reported focal solutions are projected on the lower hemisphere. Events fall

within ± 30 km for all profiles except for C-C', whose narrower width of ± 10 km is chosen to avoid oversampling due to the 1997 sequence. The shaded areas at the right side of the profiles indicate the number of events vs depth. Interpreted seismic reflection profile in proximity of B-B' (CROP-03 modified from *Finetti et al.,* 2001) is also projected. CO_2 flux is from data of *Chiodini et al*. [2004] and 500°C isotherm is from *Della Vedova et al.* [2001]. For the Adriatic and Tyrrhenian isobaths see Fig. 2 and corresponding caption.

Figure 5. Depth distribution of the seismicity of Fig. 1 on the cross-sections D-D' and E-E' shown in Fig. 2. The reported focal solutions are projected on the lower hemisphere. Events fall within ± 30 km. The shaded areas at the right side of the profiles indicate the number of events vs depth. Interpreted seismic reflection profile in proximity of E-E' [CROP-04 modified from *Merlini and Cippitelli, 2001*] is also projected. CO_2 flux is from data of *Chiodini et al*. [2004] and 500°C isotherm is from *Doglioni et al.* [1996]. For the Adriatic and Tyrrhenian isobaths see Fig. 2 and corresponding caption.

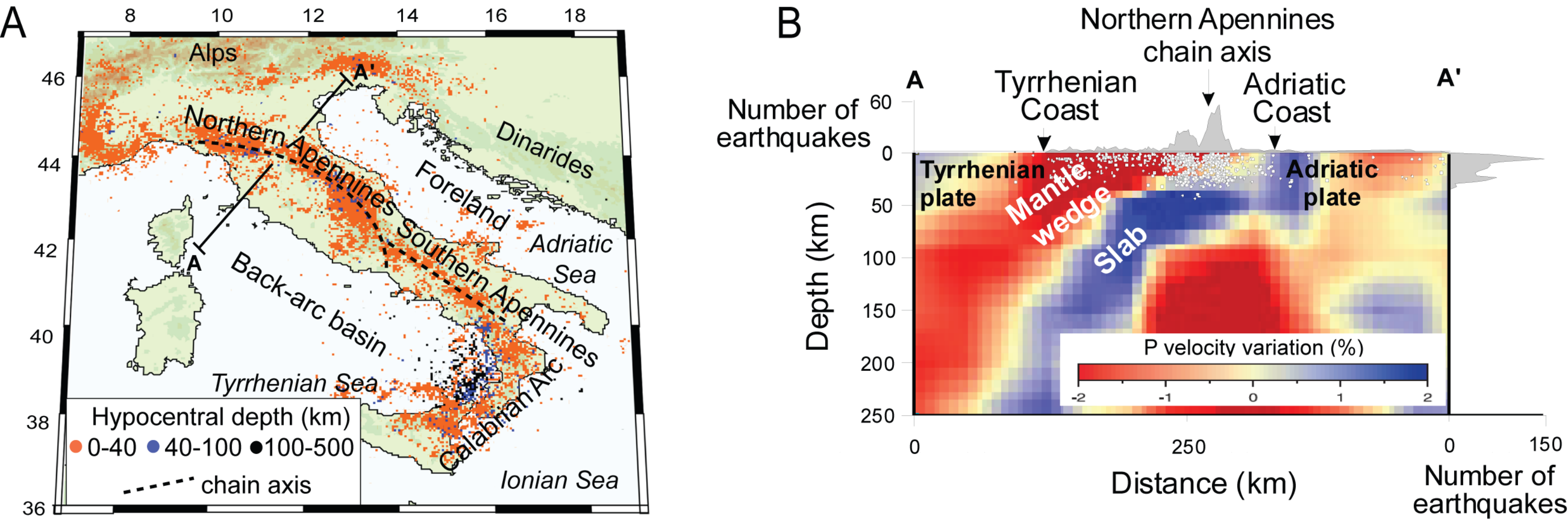
A
8
10
12
14
16
18
46
44
42
40
38
36
Alps
A'
A
Northern Apennines
Dinarides
Foreland
Adriatic
Sea
Southern Apennines
Back-arc basin
Tyrrhenian Sea
Calabrian Arc
Ionian Sea
Hypocentral depth (km)
0-40
40-100
100-500
chain axis
B
Northern Apennines
chain axis
Tyrrhenian
Coast
Adriatic
Coast
A
A'
Number of
earthquakes
60
0
Tyrrhenian
plate
Mantle
wedge
Slab
Adriatic
plate
Depth (km)
50
100
150
200
250
P velocity variation (%)
-2
-1
0
1
2
0
250
Distance (km)
0
150
Number of
earthquakes

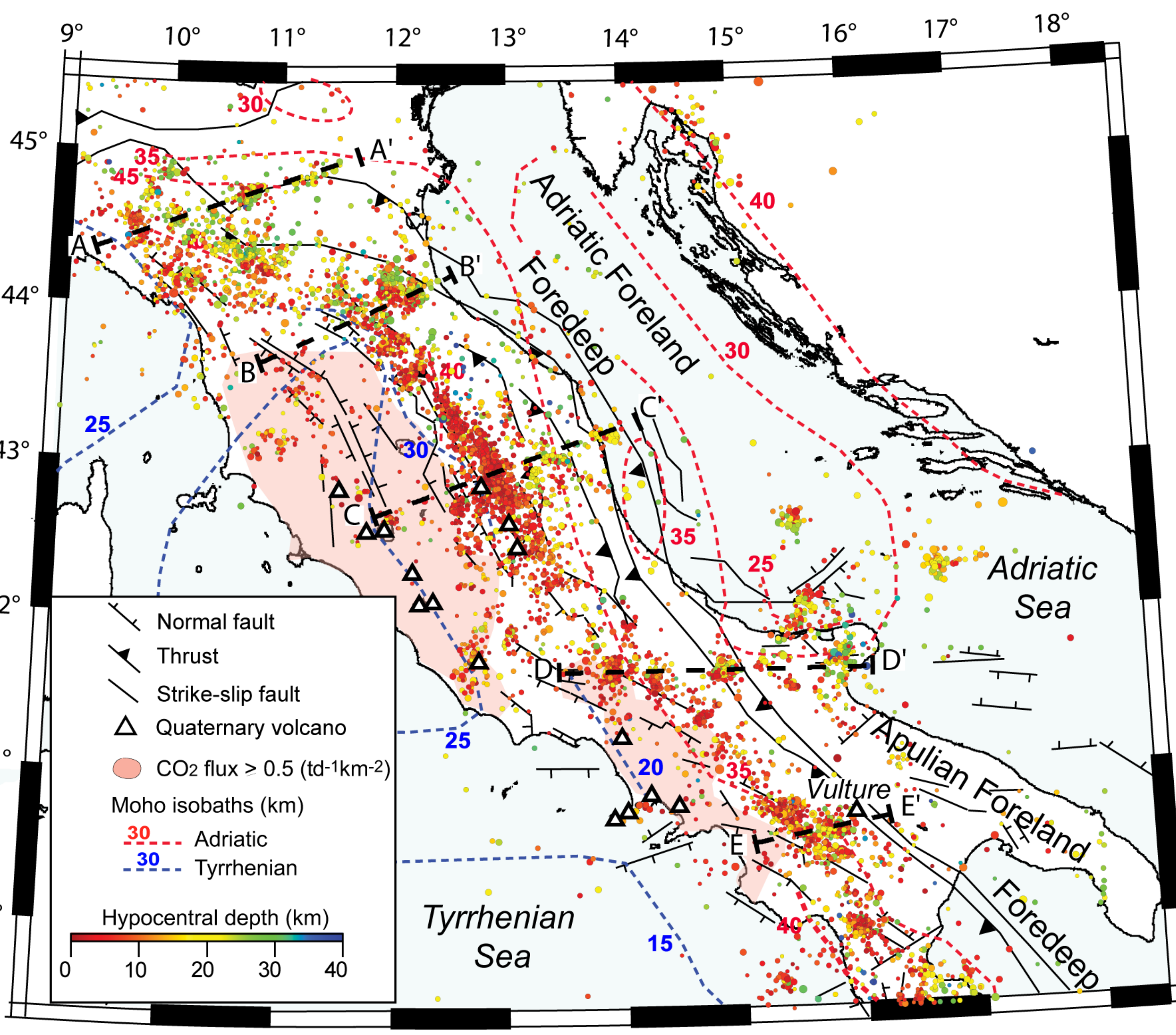
9°
10°
11°
12°
13°
14°
15°
16°
17°
18°
45°
44°
43°
42°
41°
40°
A
A'
B
B'
C
C'
D
D'
E
E'
Adriatic Foreland
Foredeep
Adriatic Sea
Apulian Foreland
Foredeep
Vulture
Tyrrhenian Sea
30
35
45
40
40
30
35
25
35
40
25
30
25
20
15
Normal fault
Thrust
Strike-slip fault
Quaternary volcano
CO2 flux ≥ 0.5 (td-1km-2)
Moho isobaths (km)
30 Adriatic
30 Tyrrhenian
Hypocentral depth (km)
0
10
20
30
40

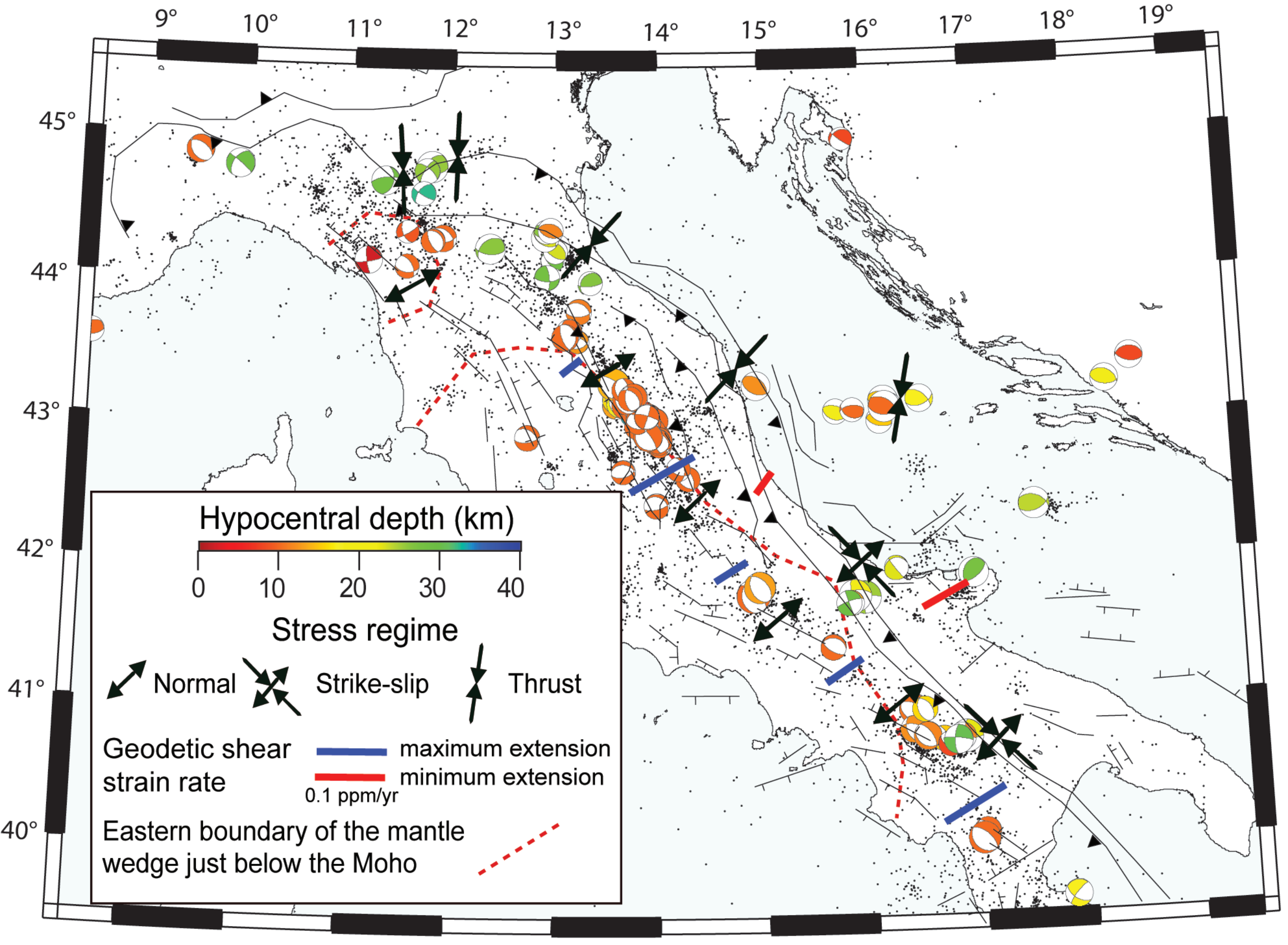

9°
10°
11°
12°
13°
14°
15°
16°
17°
18°
19°
45°
44°
43°
42°
41°
40°
Hypocentral depth (km)
0
10
20
30
40
Stress regime
Normal
Strike-slip
Thrust
Geodetic shear strain rate
maximum extension
minimum extension
0.1 ppm/yr
Eastern boundary of the mantle wedge just below the Moho

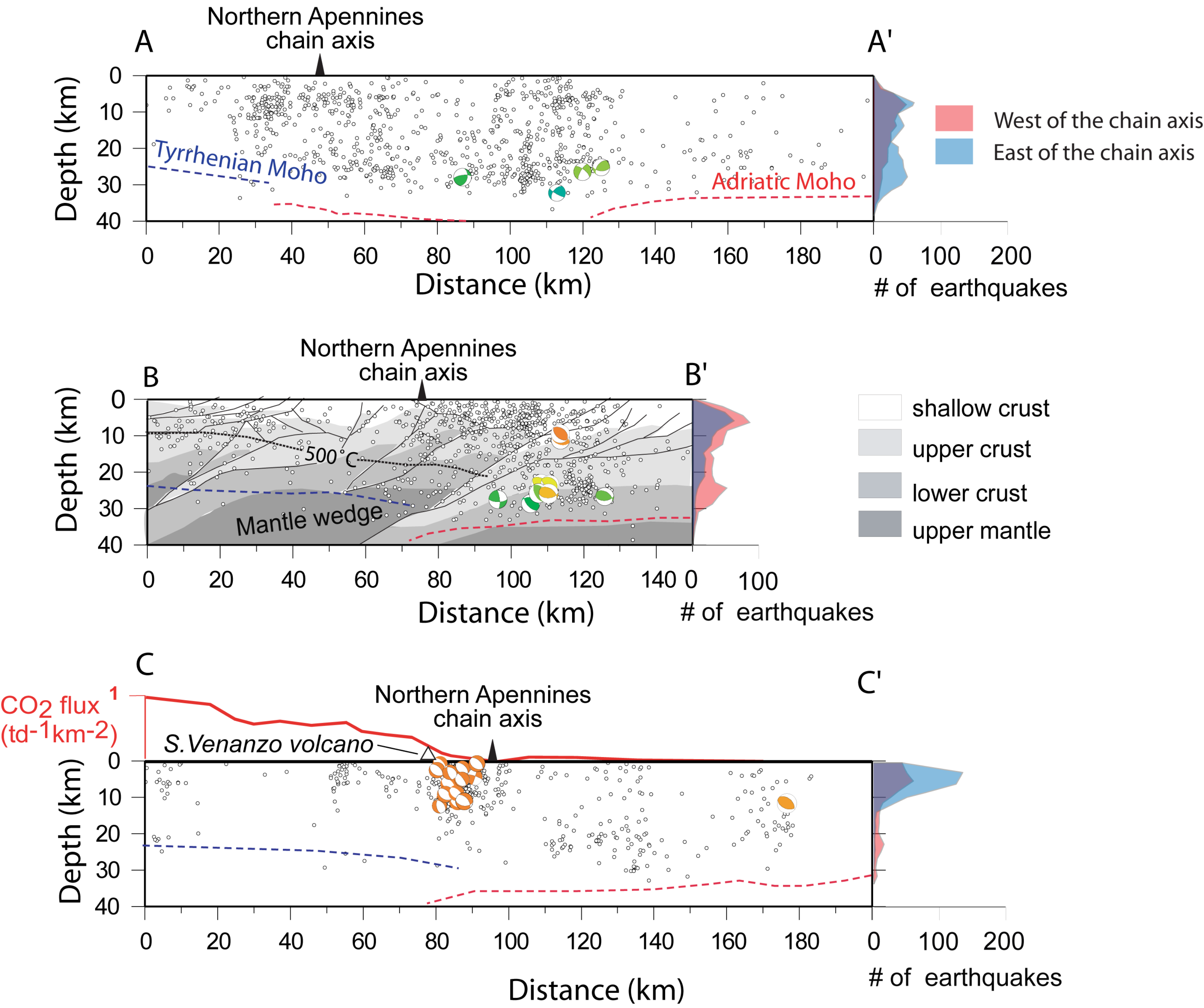

A
Northern Apennines chain axis
A'
Depth (km)
Tyrrhenian Moho
Adriatic Moho
Distance (km)
# of earthquakes
West of the chain axis
East of the chain axis
B
Northern Apennines chain axis
B'
500°C
Mantle wedge
shallow crust
upper crust
lower crust
upper mantle
C
C'
CO2 flux (td-1km-2)
S.Venanzo volcano
Northern Apennines chain axis

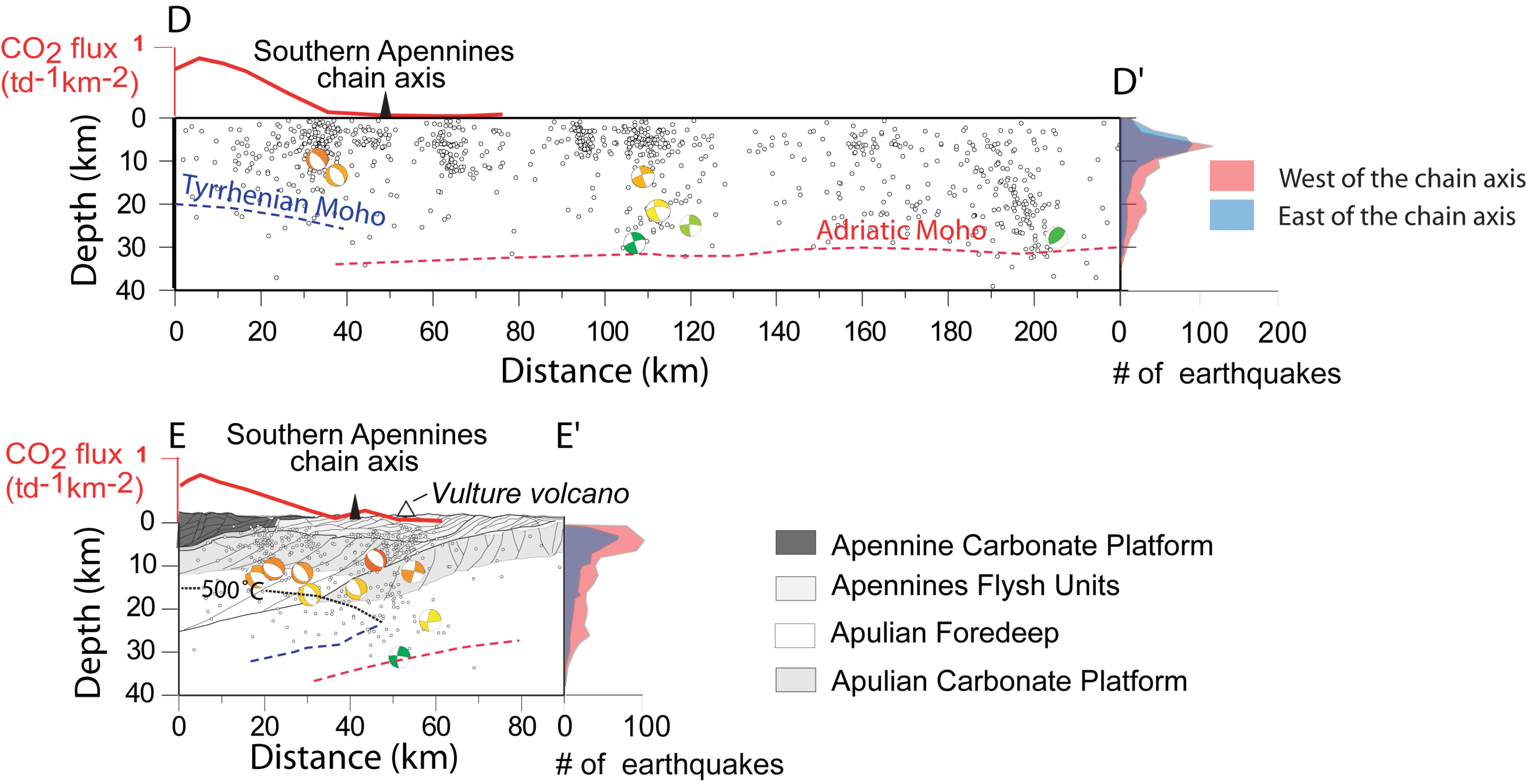

D
CO2 flux 1
(td-1km-2)
Southern Apennines
chain axis
D'
Depth (km)
0
10
20
30
40
Tyrrhenian Moho
Adriatic Moho
0
20
40
60
80
100
120
140
160
180
200
Distance (km)
0
100
200
# of earthquakes
West of the chain axis
East of the chain axis
E
CO2 flux 1
(td-1km-2)
Southern Apennines
chain axis
Vulture volcano
E'
500°C
Depth (km)
0
10
20
30
40
0
20
40
60
80
Distance (km)
0
100
# of earthquakes
Apennine Carbonate Platform
Apennines Flysh Units
Apulian Foredeep
Apulian Carbonate Platform